We are IntechOpen,
the world's leading publisher of
Open Access books
Built by scientists, for scientists

6,900
Open access books available

186,000
International authors and editors

200M
Downloads

Our authors are among the

154
Countries delivered to

TOP 1%
most cited scientists

12.2%
Contributors from top 500 universities

CLARIVATE ANALYTICS
BOOK CITATION INDEX
INDEXED

WEB OF SCIENCE™

Selection of our books indexed in the Book Citation Index
in Web of Science™ Core Collection (BKCI)

Interested in publishing with us?
Contact book.department@intechopen.com

Numbers displayed above are based on latest data collected.
For more information visit www.intechopen.com

Chapter

Optimization of Lift-Curve Slope for Wing-Fuselage Combination

Vladimir Frolov

Abstract

The paper presents results obtained by the author for wing-body interference. The lift-curve slopes of the wing-body combinations are considered. A 2D potential model for cross-flow around the fuselage and a discrete vortex method (DVM) are used. Flat wings of various forms and the circular and elliptical cross sections of the fuselage are considered. It was found that the value of the lift-curve slopes of the wing-body combinations may exceed the same value for an isolated wing. An experimental and theoretical data obtained by other authors earlier confirm this result. Investigations to optimize the wing-body combination were carried within the framework of the proposed model. It was revealed that the maximums of the lift-curve slopes for the optimal midwing configuration with elliptical cross-section body had a sufficiently large relative width (more than 30% of the span wing). The advantage of the wing-fuselage combination with a circular cross section over an isolated wing for wing aspect ratio greater than 6 can reach 7.5% at the relative diameter of fuselage equal to approximately 0.2.

Keywords: wing-fuselage combination, lift-curve slope, discrete vortex method, 2D potential cross-flow model, optimization

1. Introduction

An analysis of a lift-curve slope for wing-fuselage combinations currently plays an important role in studies of aerodynamics and the preliminary design of a modern aircraft.

Since the aircraft occurrence aircraft designers have been interested in the problems of the wing-body interference in aviation and missile technology. Initially, research is focused on the experimental study of specific wing-body combinations [1–6]. First mathematical models of the wing-fuselage interference were offered later. The solution of the linearized problem of the ideal incompressible flow around arbitrary shape wings in the presence of the fuselage is a difficult task since it is necessary to solve the three-dimensional Laplace equation for the velocity potential which satisfies the boundary conditions on the surface of the wing-body combination and the boundary conditions at infinity. One of the few exact solutions was obtained by Golubinsky in the article [7]. The first theoretical calculations were based on the inversion of discrete vortices inside the cross-section body [8], on the solution of integral equations [9], on the application the thin body theory [10–21] or the strip method [14, 15, 22], and on the application of the velocity potential [23–26] or the stream function [27] written in the Trefftz's plane. The application of

the velocity potential in the Trefftz's plane [22–26, 28–30] gives the opportunity to get the distribution of lift along the wingspan. Let us pay attention to one important result that was first theoretically obtained by Multhopp and presented in a review by Ferrari [22]. It is important to note that this fact was experimentally confirmed by Jacobs and Ward [1]. This result shows that the value of the lift-curve slope of the wing-body combination at a certain relative value diameter of the fuselage $\overline{D} = d_f/b$ (b is the wingspan; d_f is the diameter of the fuselage) exceeds the same value for the isolated wing of the same geometry which is used in the wing-fuselage configuration. Let us give some examples confirming this fact. For the scheme of midwing monoplane with cylindrical fuselage $\overline{D} = 0.14$ and trapezoidal wing with aspect ratio $AR = 4.83$ and taper ratio $\lambda = 2, 38$, the value of the lift-curve slope of the wing-body combination $C_{L_\alpha W, \text{B}}$ exceeds the same value $\overline{C}_{L_\alpha W}$ for the isolated wing of the same geometry which is used in the wing-body configuration by approximately 5% (4.75%, an experiment; 4.92%, theory) [22]. For the wing-body combination No. 13 in the experimental Jacobs and Ward's paper [1], the relative increase in the value of the lift-curve slope of the wing-fuselage combination was slightly greater ($\approx 6.49\%$) than the isolated wing of the same geometry, which was obtained also. In Korner's book [6], it was noted that the value of the lift-curve slope of the wing-body combination is approximately 5% higher than the same value for the wing alone. In the theoretical papers [31, 32], the excess value of the lift-curve slope of the wing-body combination above the same value for the isolated wing of the same geometry was also noted. In paper [32] the midwing monoplane scheme has received an increase in the value of the lift-curve slope of the wing-fuselage combination compared with the isolated wing with the same geometry approximately 19%. Theoretical results of the calculation value of the lift-curve slope of the wing-body combination are devoted also in papers [33–35] and book [36]. Woodward in papers [37, 38] investigated the aerodynamic characteristics of wing-fuselage combinations using the panel method. The same panel method was used in the paper [39]. An experimental study of wing-body-tail combinations was performed in the work [40].

This chapter by no means covers all papers on the interference of the wing and fuselage. Author's book [41] and paper [42] contain more detailed bibliography on the problems of the lift of the wing-body combination.

The main purpose of this paper is to give results of solving optimization problems for the values of the lift wing-body configurations and to demonstrate the conformity of computational author's results with the known experimental and theoretical results of other authors.

2. The calculation method of the interference for wing-fuselage combination

The calculation method of the interference for the wing-fuselage combination [42] includes two methods: (1) a discrete vortex method (DVM) for the surface of the wing and (2) 2D potential model of the flow for cross-flow around fuselage [41].

The original three-dimensional problem (**Figure 1**) is divided into two parts. First part is the two-dimensional problem of the flow around the cross section of the fuselage (**Figure 2**), and the second part is a three-dimensional problem for the isolated wing. In the 2D problem, the flow around the cross section of the fuselage adds a pair of discrete point vortices. The added vortices are the consequence of lift on the wing. According to Zhukovsky's theory about the lift of the wing, any lifting surface can be replaced by an equivalent П-shaped vortex; free vortices at low angles of attack lie in the plane of the wing and extend to infinity. In our model, it is
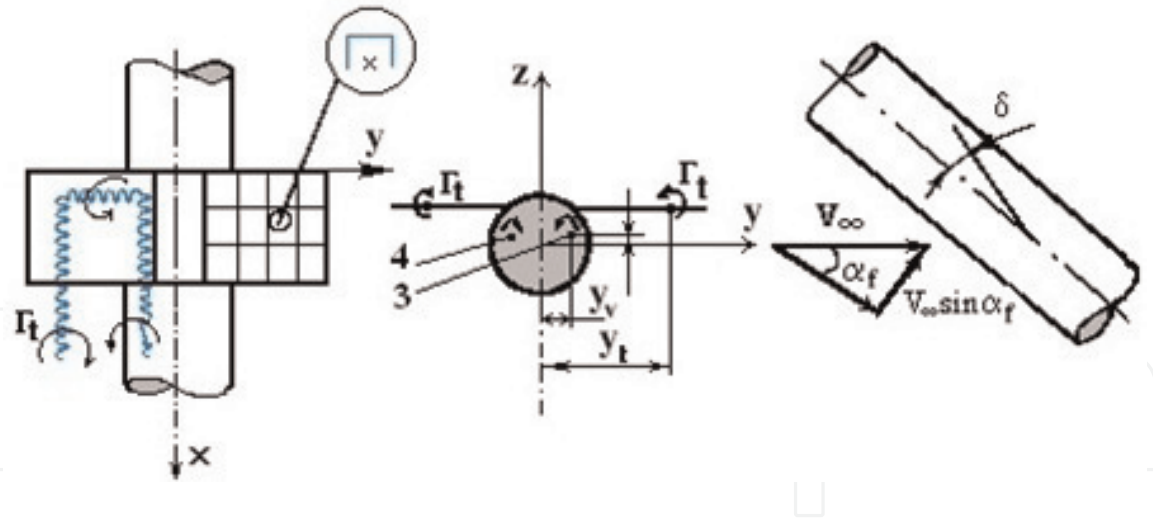
Figure 1.
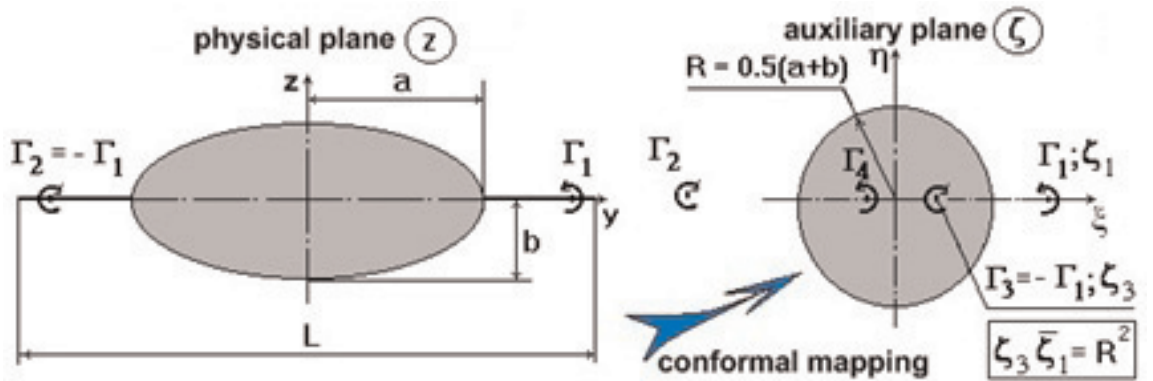*The mathematical model of wing-body interference.*

Figure 2.
The mathematical model of the potential flow around the elliptical cross section of the fuselage in the present pair of vortices.

proposed each console part of the wing replaces one Π-shaped vortex lying in the plane of the wing. The Π-shaped vortex in the left-wing console is shown in **Figure 1**. The coordinate of the free vortex and its intensity can be found from the bond equation; after the lift-isolated wing by DVM will be defined. The inversion method (**Figure 2**) can be used to satisfy the boundary conditions of impermeability on the surface of the body cross section for the canonical body, and for the arbitrary two-dimensional cross section can use the panel method. An example solution for the potential flow around the elliptical cross section of the fuselage in the present of the pair vortices is shown in **Figure 3**.

In this formulation, the problem is reduced to solving the following system of algebraic linear equations:

$$\sum_{i=1}^{L} \mathbf{\Gamma}_i \left(A_{ij} \cdot \mathbf{n}_j \right) = -\left(\mathbf{F}_j \cdot \mathbf{n}_j \right), \quad j = 1, \dots L, \tag{1}$$

where L is the number of control points (collocation points) equal to the number of attached vortices on the right-wing console, $\mathbf{n}_j$ is the unit normal vector to the jth control point on the surface of the wing, A_{ij} is the matrix of the aerodynamic influence or the matrix of the induced velocities at the control points of the wing surface from all system of horseshoe vortices (left and right consoles for the isolated wing), and $\mathbf{F}_j$ is a column vector of the velocity induced in the jth the control point on the wing surface by incoming flow and the flow from the cross section of the fuselage that includes
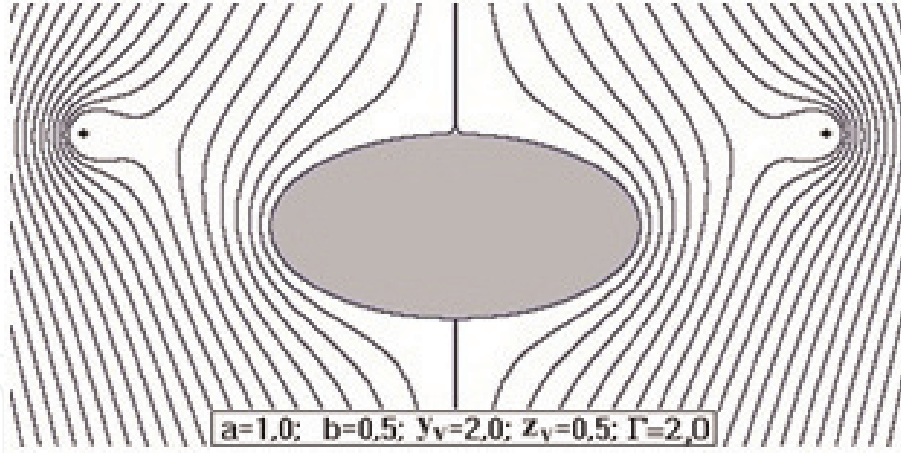
a=1.0; b=0.5; y_v=2.0; z_v=0.5; Γ=2.0

Figure 3.
Streamlines of the potential flow around the elliptical cross section of the fuselage in the present pair of vortices.

either inversion of the vortices or sources and sinks providing satisfying conditions impermeability on the surface body from the free vortices left and right wing.

For small angles of attack of the wing-body combination ($\alpha \ll 1$) and small wing deflection angle (angle of inclination wing), ($\delta \ll 1$) can use the linear formulation, and then a solution can be written as a linear function of the angle of attack and wing deflection angle:

$$\Gamma_i = \Gamma_i^{\alpha} \cdot \alpha + \Gamma_i^{\delta} \cdot \delta. \tag{2}$$

Right parts of the system of algebraic linear equations Eq. (1) can be represented also as

$$\mathbf{F}_j = \mathbf{F}_j^{\alpha} \cdot \alpha + \mathbf{F}_j^{\delta} \cdot \delta. \tag{3}$$

In Eqs. (2) and (3), Γ_i^{α}, Γ_i^{δ}, $\mathbf{F}_j^{\alpha}$, $\mathbf{F}_j^{\delta}$ are derivatives of the Γ_i, $\mathbf{F}_j$ on the angle of attack α and wing deflection angle δ, respectively.

For calculating the right parts of the system Eq. (1) for the problem with the fuselage of an arbitrary cross section of the body, the panel method that leads to the solution system of algebraic linear equations (4) is proposed:

$$[\mathbf{A}] \, [\boldsymbol{\sigma}] = [\mathbf{R}], \tag{4}$$

where $\boldsymbol{\sigma}$ is a column vector

$$\boldsymbol{\sigma} = \boldsymbol{\sigma}^{\alpha} \cdot \alpha + \boldsymbol{\sigma}^{\delta} \cdot \delta. \tag{5}$$

Let us give the final formula for the components of the induced velocity, for example, for the case of the circular cross section of the fuselage in jth control point of the wing panel:

$$
\begin{aligned}
V_{nj} &= V_{zj} \cos \delta \\
&= \cos \delta \left\{ V_{\infty} \sin \alpha \left[1 + \frac{R^2 \left(y_j^2 - z_j^2 \right)}{\left(y_j^2 + z_j^2 \right)^2} \right] \right. \\
&\quad \left. - \frac{\Gamma_t}{2\pi} \left[\frac{y_j - \tilde{y}_v}{\left(y_j - \tilde{y}_v \right)^2 + \left(z_j - \tilde{z}_v \right)^2} - \frac{y_j + \tilde{y}_v}{\left(y_j + \tilde{y}_v \right)^2 + \left(z_j - \tilde{z}_v \right)^2} \right] \right\},
\end{aligned} \tag{6}
$$

where $\left(y_j, \ z_j\right)$, $\left(\tilde{y}_v, \ \tilde{z}_v\right)$ are coordinates of the control point and the inversion vortex point (see **Figure 1**), respectively, and V_{nj} is a normal component of the velocity to the surface at the jth control point wing panel induced velocity component along the OZ-axis of the cylinder in cross-flow (see **Figure 1**). Coordinate inversion vortices are defined by Milne-Thomson's theorem about the circle [43]. The coordinate y_t and intensity Γ_t of the free vortex can be found on the connection equations [41, 42, 44].

So the task of the wing-body interference is reduced to the solution Eq. (1) with the right part Eq. (6) or right-hand parts, obtained by solving the system (4) that provides the solution of the problem for the potential flow around an arbitrary contour of the panel method. The method of the successive iterations provides an agreement of the velocity field on the surface wing and the surface fuselage. Each iteration is reduced to the solution of systems of linear algebraic equations (1) with corrected right part Eq. (6). The zero iteration can select the solution for the isolated wing. For small angles of attack and wing deflection angle, the proposed model or the linear formulation allows to get the solution of two problems at once, which can be called $\alpha\alpha$-problem (fuselage and wing have the same angle of attack, angle of the wing deflection angle equal to zero) and $\delta 0$-problem (the fuselage has a zero angle of attack, and the wing has deflection angle δ not equal to zero). For this linear case, formulas for the coefficients of the normal forces of the wing and the body are of the form Eq. (7)

$$C_{L \ \text{W(B)}} = C_{L_\alpha \ \text{W(B)}}\alpha + C_{L_\delta \ \text{W(B)}}\delta,$$

$$C_{L \ \text{B(W)}} = C_{L_\alpha \ \text{B(W)}}\alpha + C_{L_\delta \ \text{B(W)}}\delta, \tag{7}$$

$$C_{L_\alpha \ \text{W, B}} = C_{L_\alpha \ \text{W(B)}} + C_{L_\alpha \ \text{B(W)}}, \quad C_{L_\delta \ \text{W, B}} = C_{L_\delta \ \text{W(B)}} + C_{L_\delta \ \text{B(W)}},$$

where values $C_{L_\delta \ W(B)}$, $C_{L_\delta \ B(W)}$, $C_{L_\alpha \ W(B)}$, $C_{L_\alpha \ B(W)}$ are obtained from the solution $\delta 0$- and $\alpha\alpha$-problem, respectively.

3. Calculation results

The comparison of the calculation results obtained from the above theoretical model with calculations by the DVM for case $\alpha\alpha$-problem [34–36] is shown in **Figures 4–9**. The rectangular, triangular, and swept wings were considered. It may be noted is enough good agreement of calculated data.

The changing of coordinates of the aerodynamic center x_{AC}/c measured from the beginning of the mean aerodynamic chord is also shown in **Figures 4**, **6**, and **8**. The coefficient of the interference K_Σ in these figures is defined by the formula

$$K_\Sigma = \frac{C_{L_\alpha \text{W, B}}}{C_{L_\alpha \text{W}}}, \tag{8}$$

where value $C_{L_\alpha \text{W}}$ is a lift-curve slope for an isolated wing composed of two consoles of this wing.

The comparison of the calculation results obtained from the above theoretical model with calculations by the numerical method of singularities for case $\delta 0$-problem [31] is presented in **Figure 10**.

The comparison of calculated data for the mathematical model described above and the calculated and experimental data of other researchers [45–49] is shown in **Figures 11–13**.
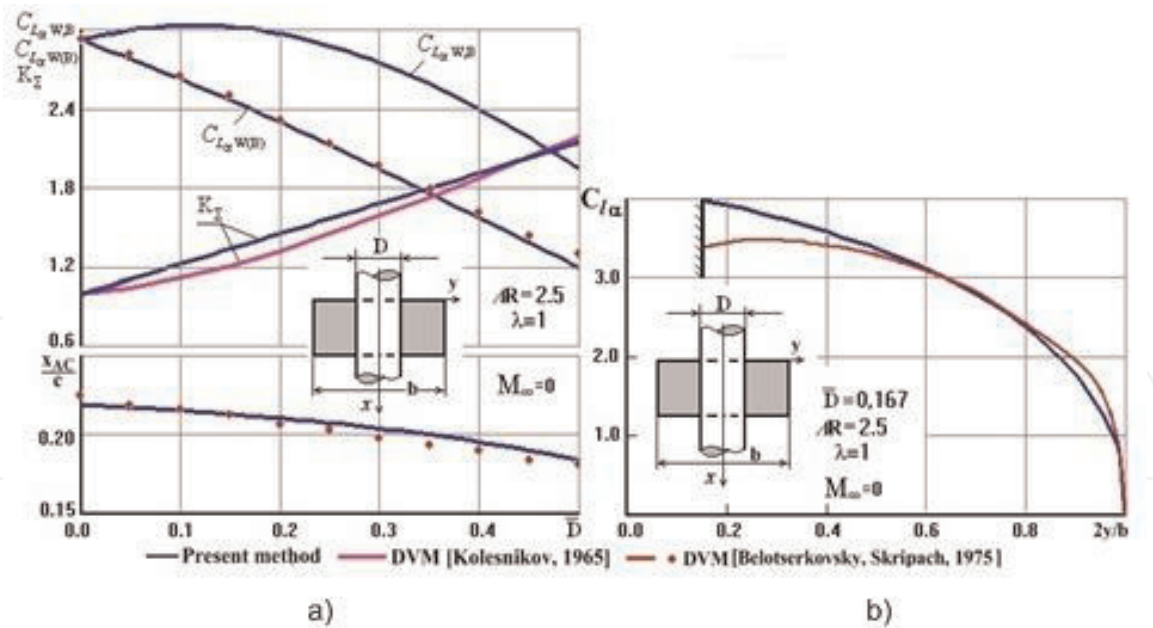
Figure 4.
The lift-curve slopes vs. relative diameter of the fuselage (a); the lift-curve slopes vs. relative span for the rectangular wing in the midwing-body combination (b).
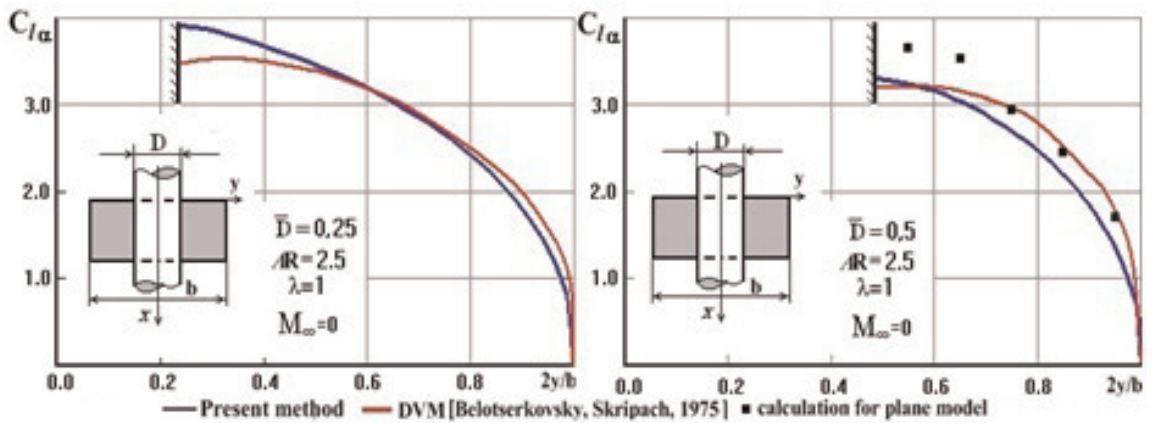

Figure 5.
The lift-curve slopes vs. relative span for the rectangular wing in the midwing-body combination.
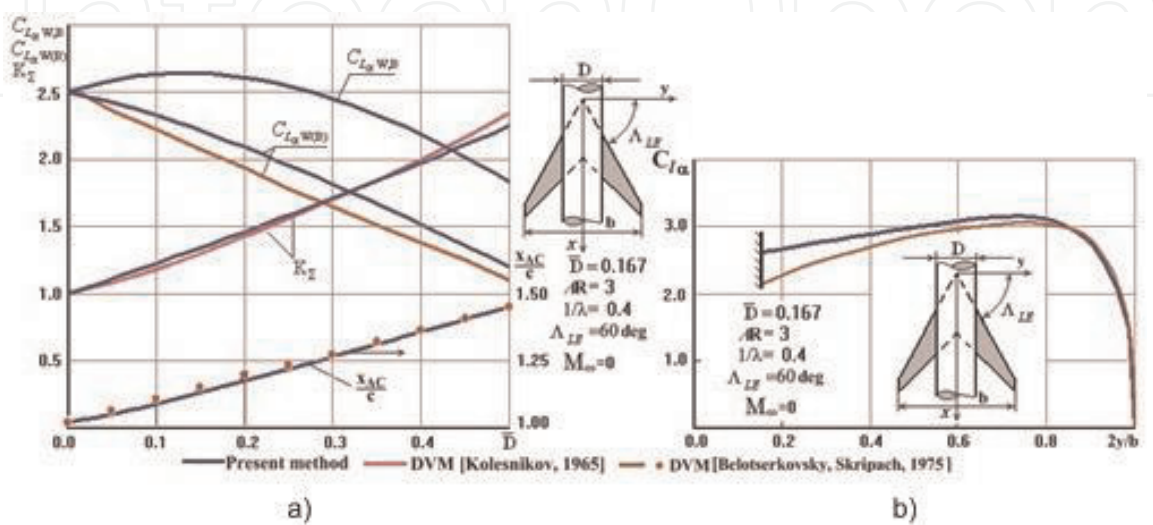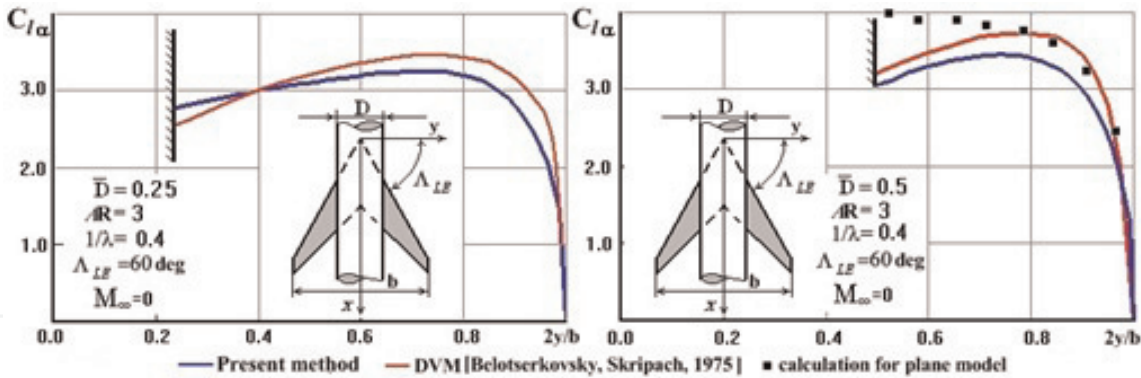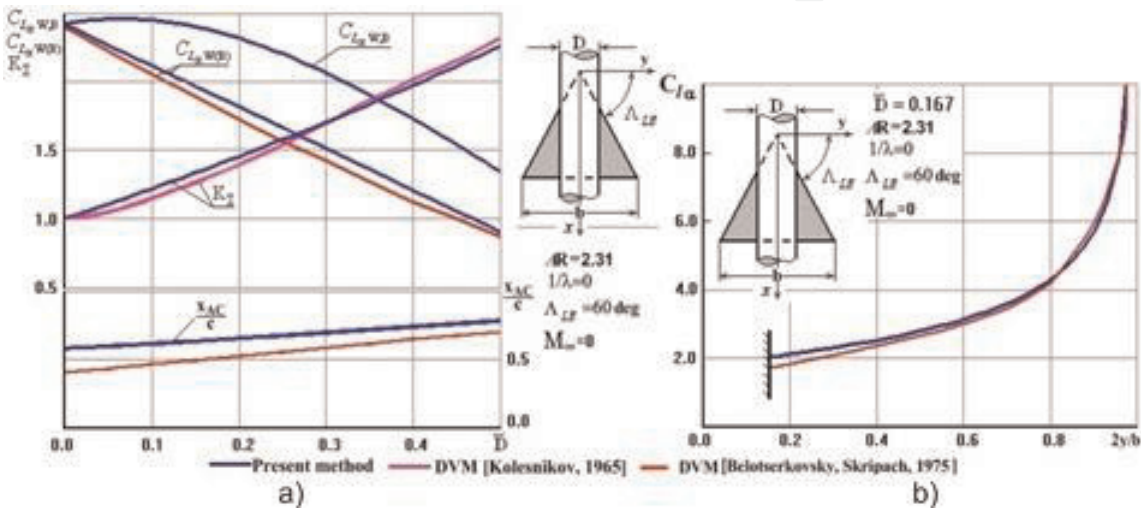

Figure 6.
The lift-curve slopes vs. relative diameter of the fuselage (a); the lift-curve slopes vs. relative span for the swept wing in the midwing-body combination (b).

Figure 7.
The lift-curve slopes vs. relative span for the swept wing in the midwing-body combination.

Figure 8.
The lift-curve slopes vs. relative diameter of the fuselage (a); the lift-curve slopes vs. relative span for the delta-shaped wing in the midwing-body combination (b).
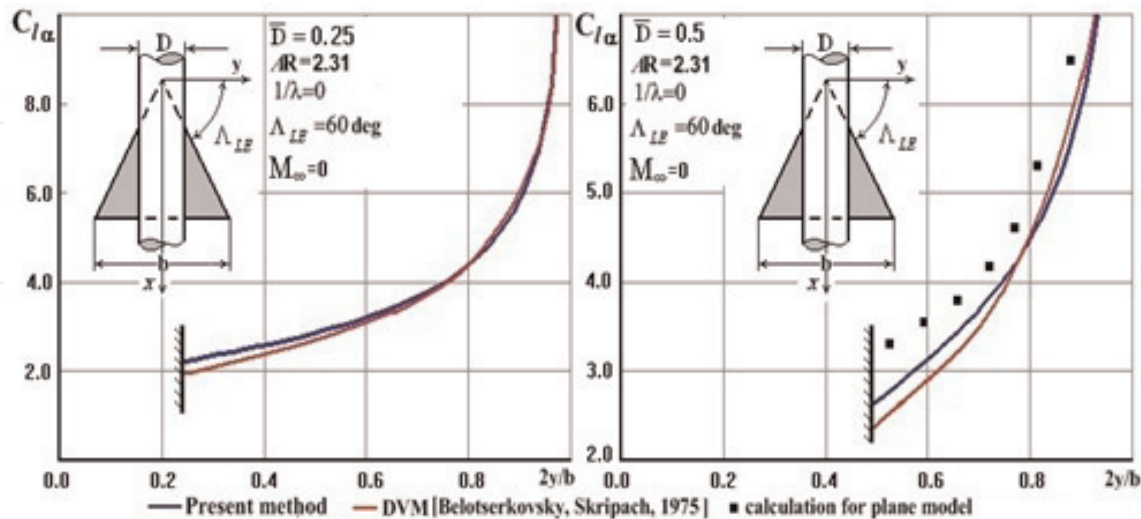

Figure 9.
The lift-curve slopes vs. relative span for delta-shaped in the midwing-body combination.

Figure 14 shows an influence of compressibility on the values of theoretical lift-curve slopes for case midwing monoplane combination with the rectangular and delta-shaped wing. **Figure 15** also shows an influence of compressibility on values of theoretical lift-curve slopes for case high-wing monoplane combination with the rectangular and delta-shaped wing [33].
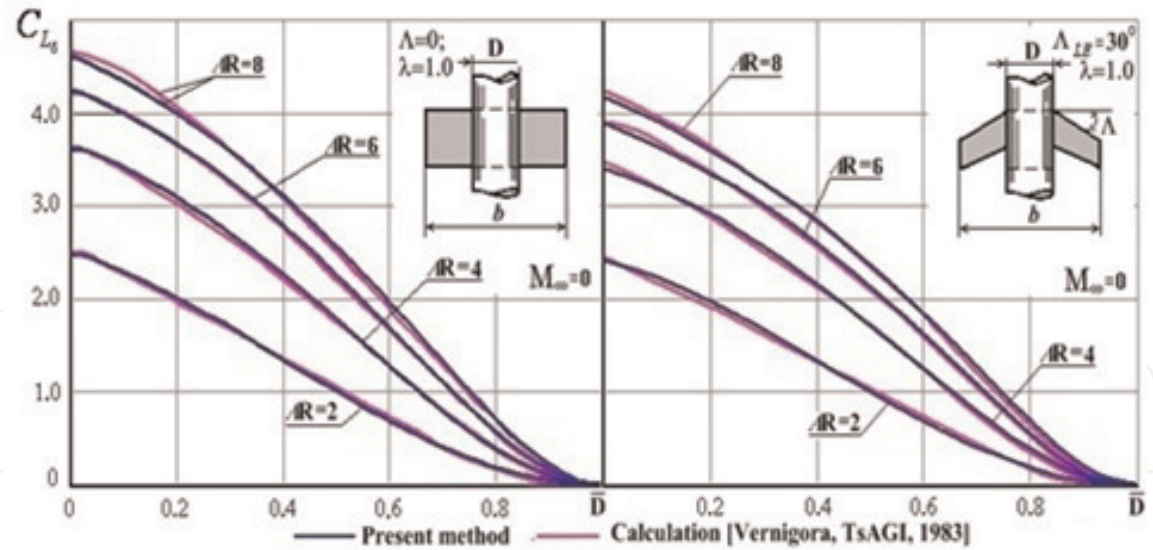
Figure 10.
The lift-curve slopes vs. relative diameter of the fuselage for case δ0-problem for midwing-body combination.
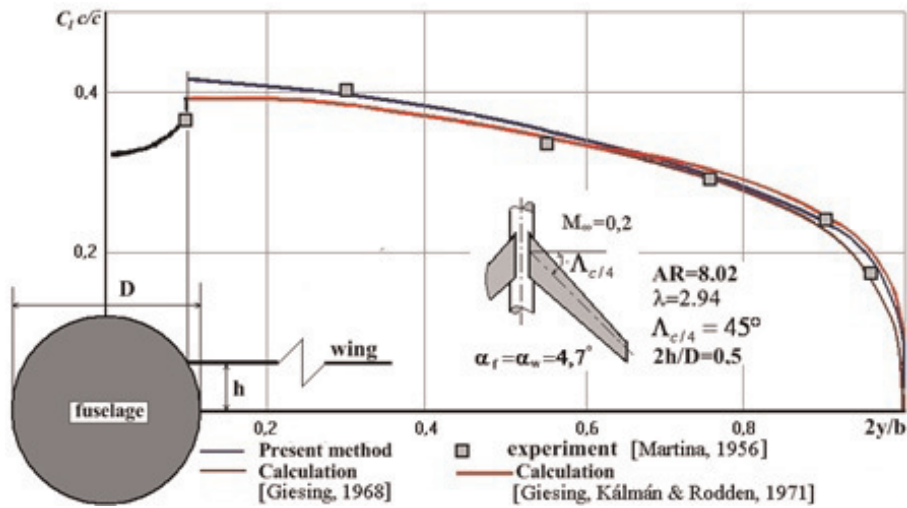

Figure 11.
The distribution lift coefficient along the relative span of the swept wing for case high-wing monoplane combination.

Of particular interest is the comparison of calculated and experimental data to prove that the lift-curve slope for the wing-body combination exceeds this value for an isolated wing. **Figure 16** shows this comparison.

The area shown in color in **Figure 16** indicates the advantage of the lift-curve slopes of the wing-body combinations over an isolated wing. Calculations and experiments show that with an increasing aspect ratio of the wing, this advantage will increase. This circumstance is important since the modern development of the aircraft industry tends to increase the aspect ratio of the wing. Another conclusion is that the maximum of the lift-curve slopes with a wing aspect ratio of 6 is achieved at relative fuselage diameter of approximately 0.2. Such a relative diameter of the fuselage allows the design of modern aircraft with a wide fuselage. Numerical studies have shown that with increasing aspect ratio of the wing and the ratio of the width to the height of the fuselage elliptical cross sections, the advantage of lift-curve slopes of the wing-body combinations over isolated wings becomes larger. The noted facts allow us to formulate and solve an optimization problem.
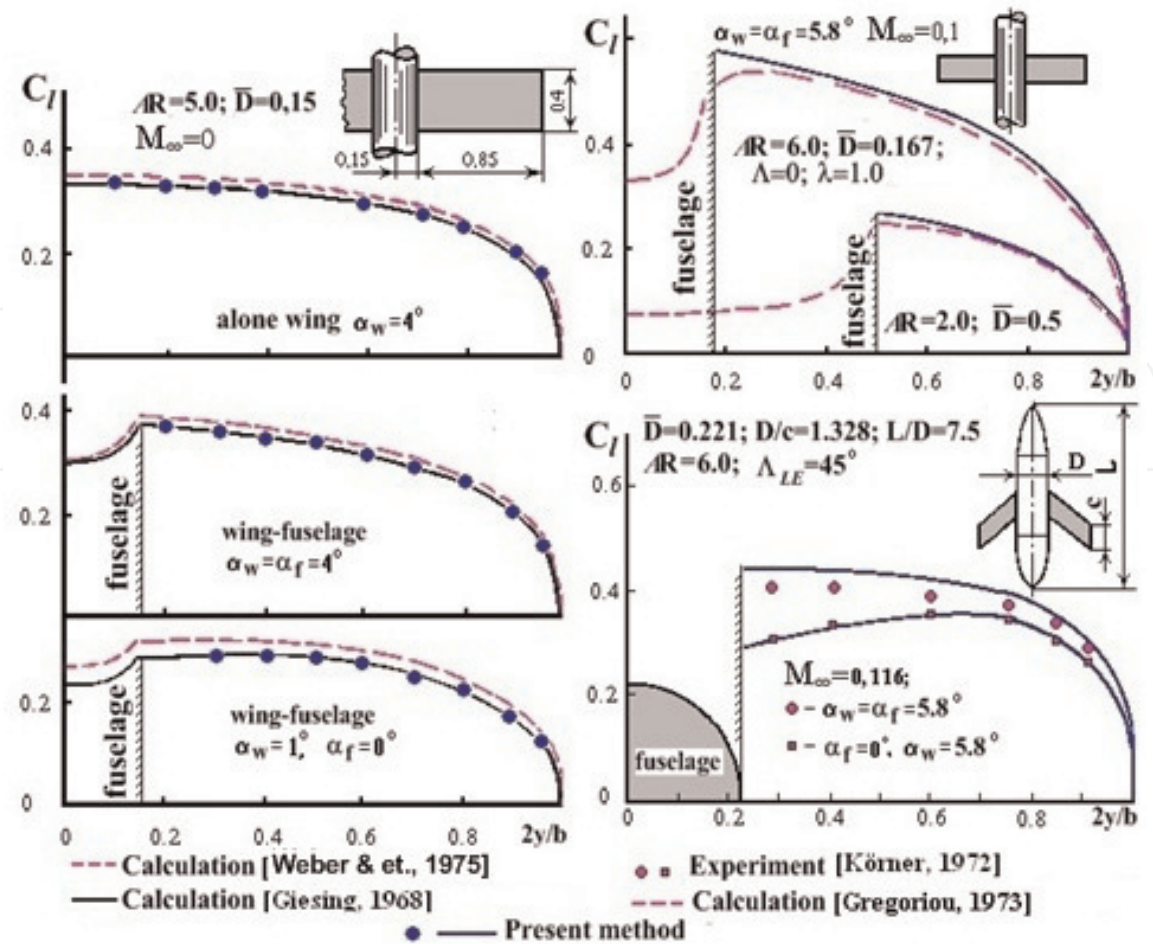
Figure 12.
The distribution lift coefficient along the relative span of the rectangular wing for case high-wing monoplane combination.
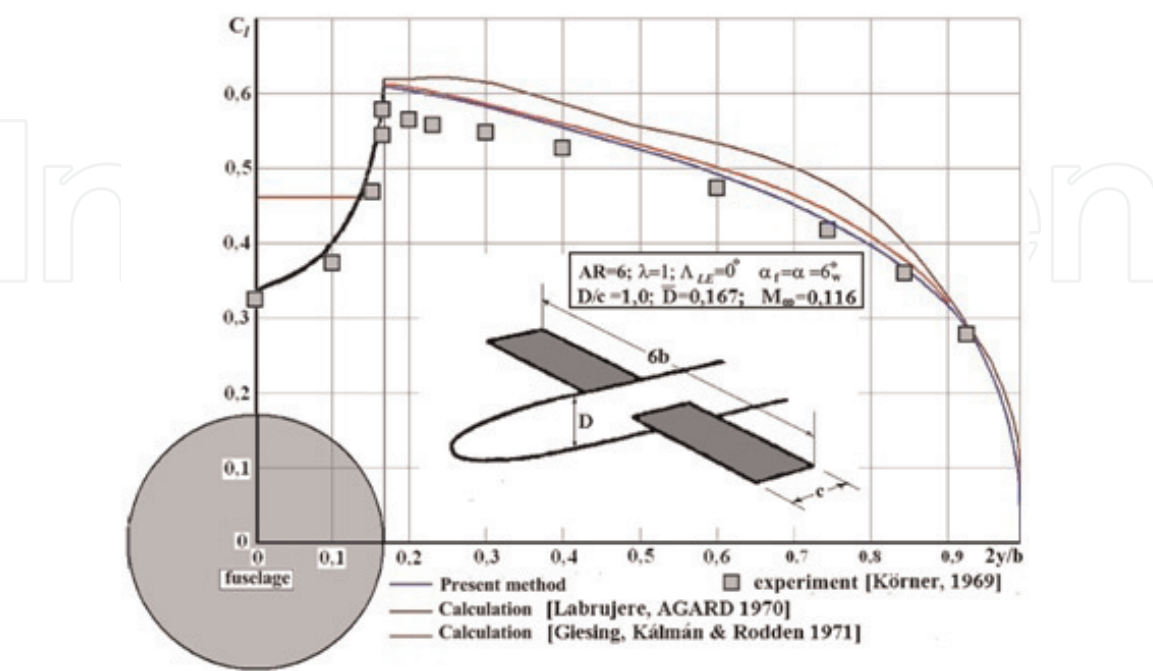

Figure 13.
The distribution lift coefficient along the relative span of the rectangular wing for case midwing monoplane combination.
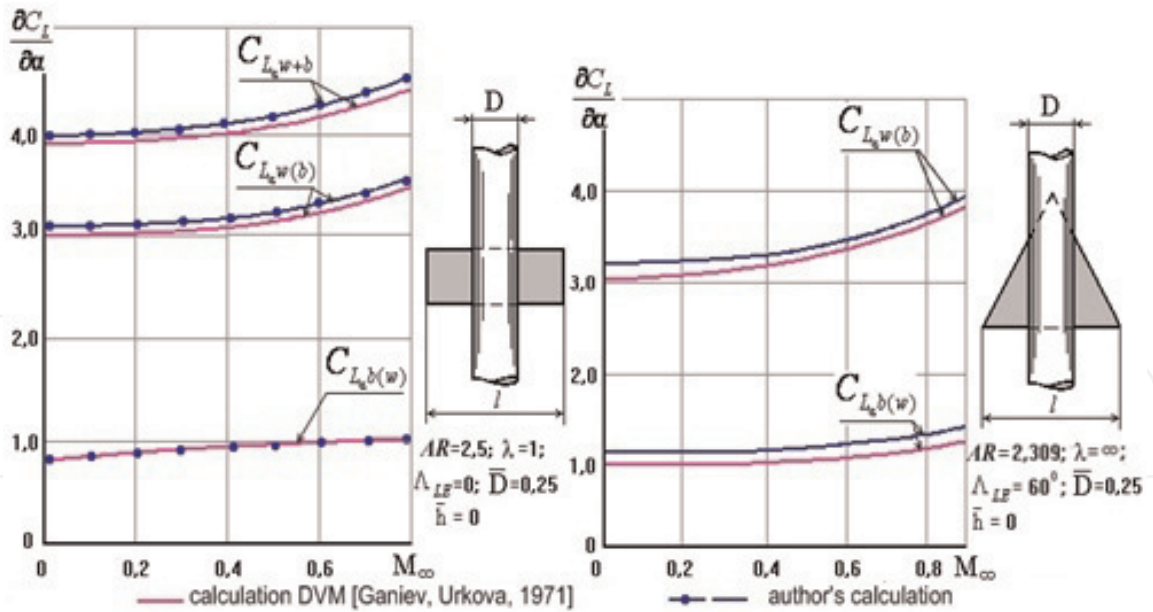
Figure 14.
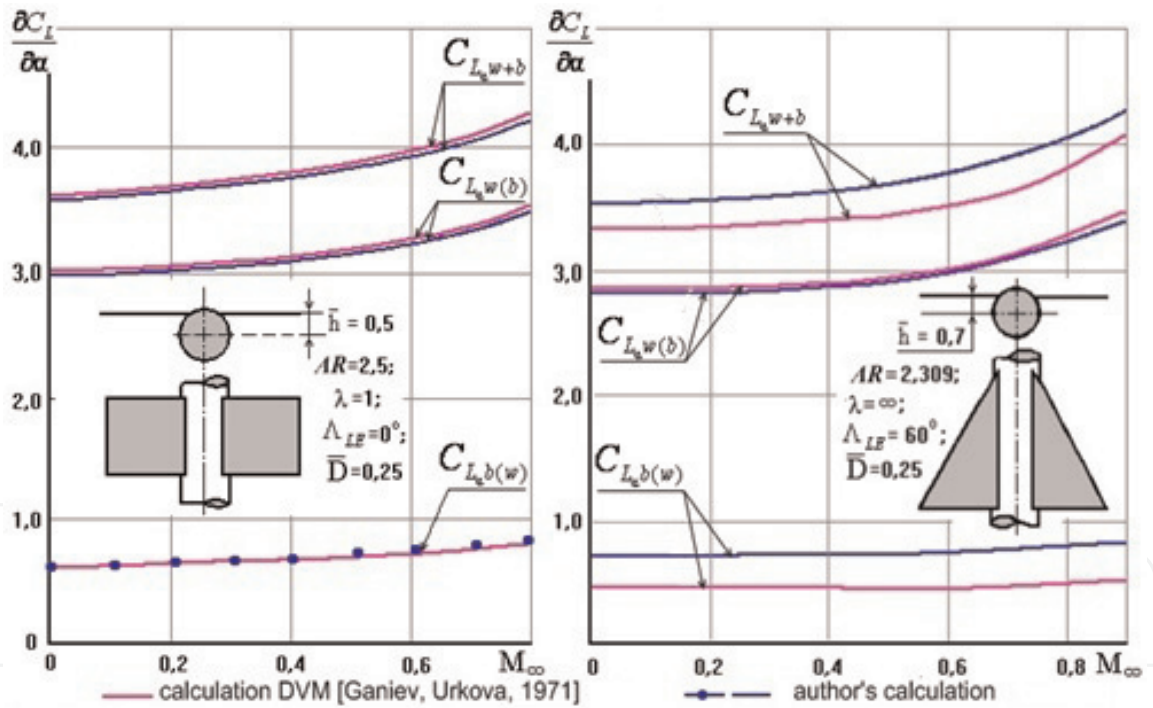*Calculation results of lift-curve slopes vs. Mach number for case midwing monoplane combination.*

Figure 15.
Calculation results of lift-curve slopes vs. Mach number for case high-wing monoplane combination.

4. The formulation of the optimization problem

Note that in some theoretical and experimental papers devoted to the wing-body interference revealed a maximum dependence $\partial C_L / \partial \alpha = f\left(d_f / b\right)$. Our calculations on the above mathematical model also confirm this fact. It was found that the maximums of lift-curve slopes for a wing-body combination depends on the shape of the wing and the cross-section shape of the fuselage. The paper presents solutions to the optimization problem for the wing-body combinations with unswept trapezoidal wings and circular or elliptical cross sections.
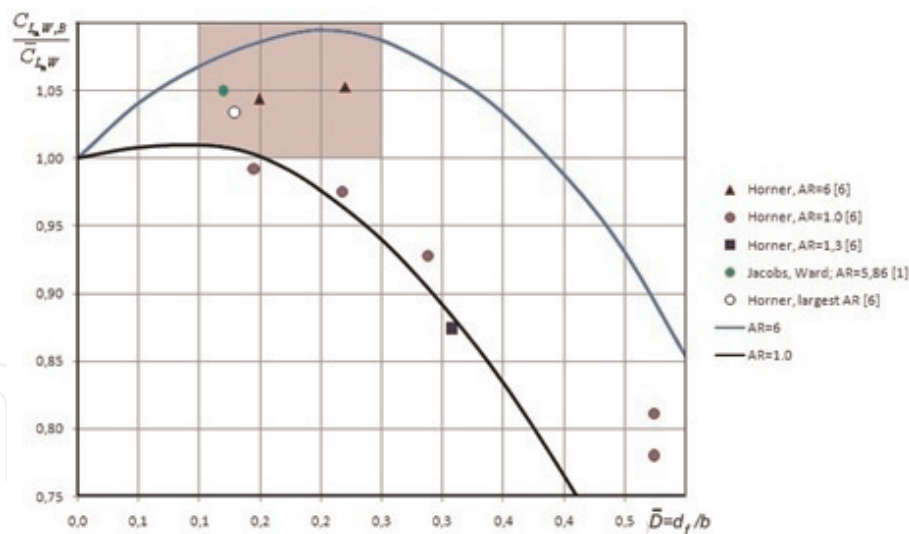
Figure 16.
Theoretical and experimental results for lift-curve slopes vs. relative diameter of the fuselage.

We will use the formulation of the optimization problem as a nonlinear programming problem as follows:

$$max \quad C_{L_\alpha W, B}(\mathbf{X}), \quad \mathbf{X} \in E^n, \tag{9}$$

where $\mathbf{X} = [x_1, x_2, 0]^T$ is a vector of the project parameters connected with geometrical characteristics of the wing-body configuration by formulates

$$\overline{D} = \frac{d_f}{b} = \frac{1}{x_1^2 + 1}, \quad \frac{1}{\lambda} = \frac{1}{x_2^2 + 1}, \tag{10}$$

where $x_1 x_2$ are auxiliary variables. The problems Eq. (9) and (Eq. (10) are a problem of unconditional optimization, for which there are $\overline{D} \in [0;1]$, $(1/\lambda) \in [0;1]$ and $x_1 \in [-\infty; +\infty]$, $x_2 \in [-\infty; +\infty]$.

5. Results of the optimization problem for lift-curve slope for midwing-body monoplane configuration

Figures 17 and **18** show results of the optimization problem for lift-curve slope for midwing-body monoplane configuration with circular cross-section fuselage vs. the aspect ratio of the rectangle wing. In **Figure 16**, the notation is used:

$$\overline{K}_\Sigma = \frac{C_{L_\alpha W, B}}{\overline{C}_{L_\alpha W}},$$

where $C_{L_\alpha W, B}$ is the lift-curve slope of the wing-body combination the same as in Eq. (9) and $\overline{C}_{L_\alpha W}$ is a lift-curve slope of the isolated wing in which it is included part of the occupied fuselage.

Figure 18 shows the results of the solution of the optimization problem for lift-curve slopes for midwing-body monoplane configuration with elliptical cross-section fuselage. Maximum values of the lift-curve slopes depend on the aspect ratio of the rectangular wing and the ratio of the axes of the ellipse. **Figure 18** shows that the advantage of the wing-fuselage combination over an isolated wing is enhanced
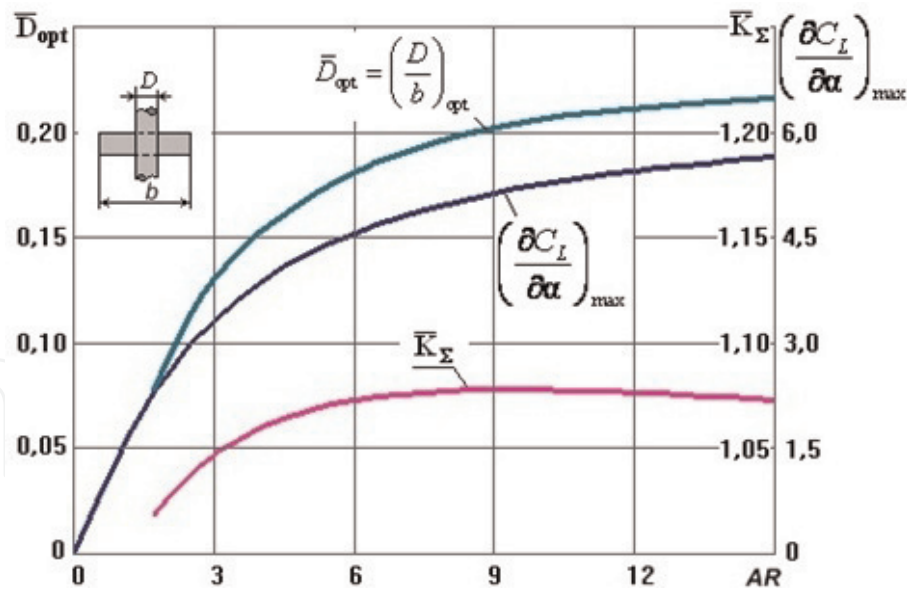
Figure 17.
The optimal relative diameter of the fuselage with circular cross-section body for the midwing configuration vs. the aspect ratio of the rectangular wing.
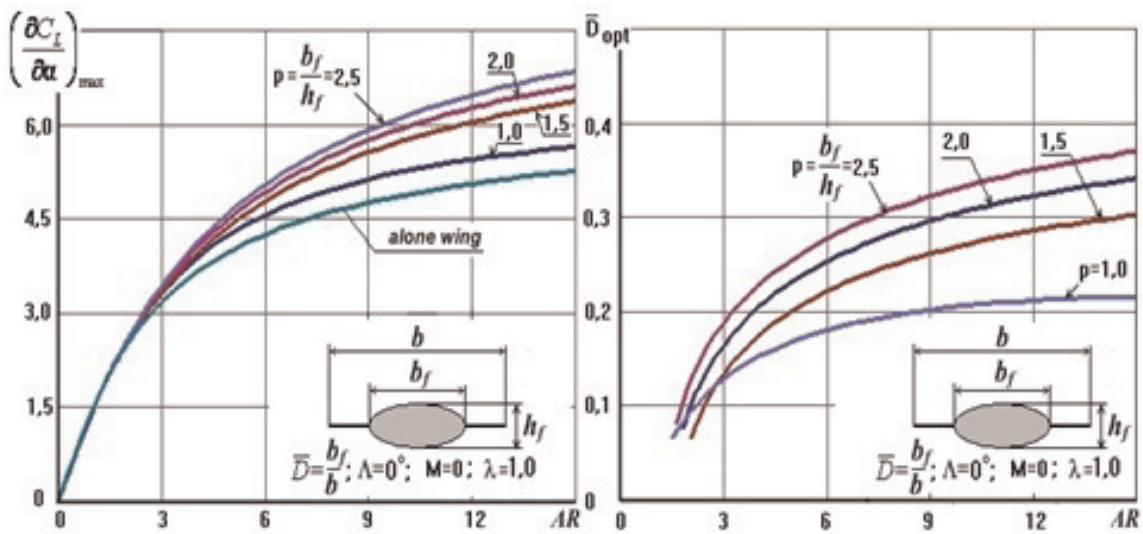

Figure 18.
Maximums of the lift-curve slopes for the optimal midwing configuration with elliptical cross-section body vs. the aspect ratio of the rectangular wing.

with increasing the aspect ratio of the rectangular wing and with increasing the ratio of the axes of the cross-section fuselage. The optimal ratio of the width of the body to the span of the wing can reach 30% and more!

Figure 19a shows the effect of the compressibility and the statistics for modern aircraft also (**Figure 19b**). Red color point shows the project of fifth-generation aircraft (project M-60, Russia). The feature of the project M-60 is a wide fuselage. As can be seen from **Figure 19b**, with the aspect ratio wing equal to 15, the optimal ratio of the width of the circular cross section to the wingspan can reach 20%!

6. Conclusions

The paper presents results obtained by the author for wing-body interference. The lift-curve slopes of the wing-body combinations are considered. A 2D potential
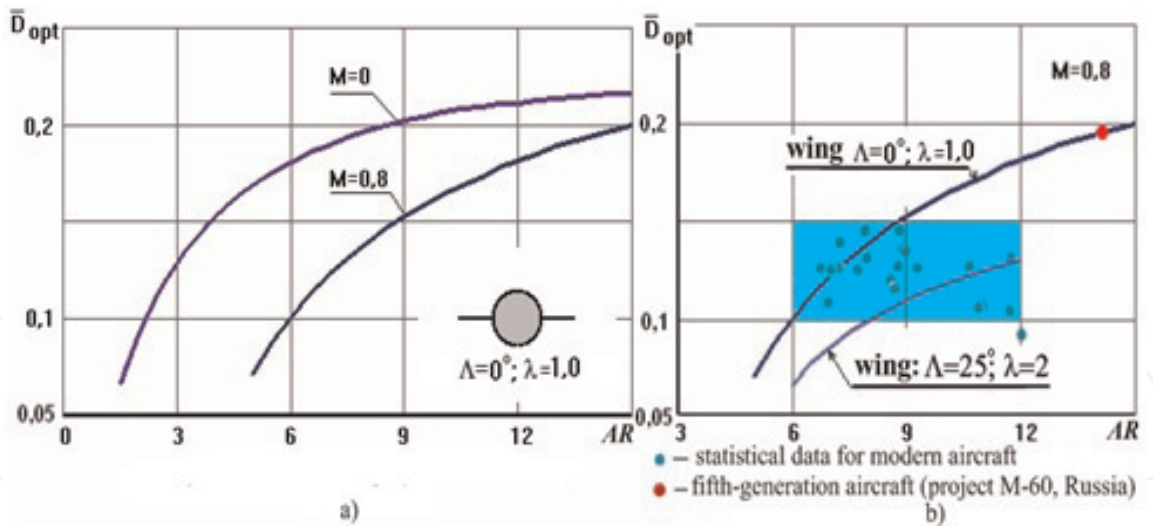
Figure 19.
Effect compressibility on the solution of the optimization problem.

model for cross-flow around the fuselage and the discrete vortex method for the wing were used. Flat wings of various forms and the circular and elliptical cross sections of the fuselage are considered. It was found that the value of the lift-curve slopes of the wing-body combinations may exceed the same value for an isolated wing. An experimental and theoretical data obtained by other authors earlier also confirms this result. Investigations to optimize the wing-body combination were carried within the framework of the proposed model. The proposed mathematical model for the solution optimization problem for the wing-body combination allows selecting the optimal geometric parameters for configuration to maximize the values of the lift-curve slopes of the wing-body combination.

It was revealed that the maximums of the lift-curve slopes for the optimal midwing configuration with elliptical cross-section body reach their values at sufficiently large relative width of the body (more than 30% of the span wing!). The advantage of the wing-fuselage combination with a circular cross section over an isolated wing at the wing aspect ratio greater than 6 can reach 7.5% at the relative diameter of fuselage equal to approximately 0.2. The advantage of the wing-fuselage combination with the elliptical cross section with the ratio of axes of the body equal to 2.5 over an isolated wing with aspect ratio equal to 12 is that it can reach 29% at relative width of fuselage equal approximately to 0.35!

Conflict of interest

The author declares no conflict of interest.

Acronyms and abbreviations

NACA	National Advisory Committee for Aeronautics
AGARD	Advisory Group for Aerospace Research and Development
ZFF	Zeitschrift für Flugwissenschaften
TsAGI	Central Aerohydrodynamic Institute
J. Aircraft	Journal of Aircraft
R&M	Reports and Memoranda
J. Aeron. Sc.	Journal of the Aeronautical Sciences
ARC CP	Aeronautical Research Council Current Papers

Author details

Vladimir Frolov
Samara National Research University, Samara, Russia

*Address all correspondence to: frolov_va_ssau@mail.ru

IntechOpen

References

[1] Jacobs EN, Ward KE. Interference of wing and fuselage from tests of 209 combinations in the N.A.C.A. Variable Density Tunnel. NACA Report; 1935. 540, p. 37

[2] Pitts WC, Nielsen JN, Kaattari GE. Lift and center pressure of wing-body-tail combinations at subsonic, transonic and supersonic speeds. NACA Report; 1957. 1307, p. 70

[3] Schneider W. Experimental investigation of wing-body interferences in the mach number range from 0.5 to 2.0. Transonic Aerodynamics. AGARD CP No. 35; Göttingen, Germany: Aerodynamische Versuchsanstalt Göttingen; 1968. pp. 20-1-20-23

[4] Kirby DA, Hepworth AG. Low-speed wind-tunnel tests on some slender airbus configurations. R&M; 1971. No. 3747, p. 55

[5] Körner H. Berechnung der potentialtheoretischen Strömung um Flügel-Rumpf-Kombinationen und Vergleich mit Messungen. ZFF; Vol. 20. 1972. pp. 351-368

[6] Korner SF, Borst HV. Fluid-Dynamic Lift. 2d ed. Published by Mrs. L.A; 1985. Hoerner, 482 p

[7] Golubinsky AI. Exact solution of interference problem of wing with fuselage at subsonic flow. In: Proceedings TsAGI; 1961. 810, pp. 23-36

[8] Lebedev BF. Approximate method of calculating load distribution on wing and fuselage at subsonic speeds. In: Proceedings TsAGI; 1958. p. 719

[9] Dorodnitsyn AA. Influence of fuselage on distribution of loads on wing span. In: Proceedings TsAGI; 1944. p. 546

[10] Keldysh VV. Interference of flat swept low-aspect ratio wing and body. In: Proceedings TsAGI; 1959. 759, pp. 1-23

[11] Keldysh VV. Lift small aspect ratio wing with body. In: Scientists Note TsAGI; VI, 5; 1975. pp. 15-28

[12] Keldysh VV. Lift and longitudinal moment of low-aspect ratio wing with body of rotation located near it. In: Scientists Note TsAGI; VIII, 3; 1977. pp. 19-31

[13] Flax AH. Comment on "correlation of wing-body combination lift data". Journal of Aircraft. 1974;**11**(5):393-394

[14] Flax AH. Integral relations in linearized theory of wing-body interference. Journal of the Aeronautical Sciences. 1953;**20**(7):483-490

[15] Flax AH, Lawrence HR. The aerodynamics of low-aspect-ratio wings and wing-body combinations. In: Third Anglo-American Aeron. Conf. Brighton; 1951; pp. 363-398, 398A-398J

[16] Lawrence HR, Flax AH. Wing-body interference at subsonic and supersonic speeds—Survey and new development. Journal of the Aeronautical Sciences. 1954;**21**(5):289-324

[17] Nielsen JN. Missile Aerodynamics. New York-Toronto-London: McGraw-Hill Book Company, Inc.; 1960. 450 p

[18] Spreiter JR. Aerodynamic properties of slender wing-body combination at subsonic, transonic and supersonic speeds. NACA TN; 1948. 1662

[19] Spreiter JR. Aerodynamic properties of the cruciform wing and body combinations at subsonic, transonic, and supersonic speeds. NACA TN; 1949. 1897

[20] Spreiter JR. Aerodynamic forces on slender plane and cruciform wing and body combinations, NACA Report. 1950. 962, pp. 271-287

[21] Spreiter JR, Sacks AH. A theoretical study of the aerodynamics of slender cruciform-wing arrangements and their wakes. NACA Report; 1956. 1296, pp. 81-106

[22] Ferrari C. Aerodynamic components of aircraft at high speeds vol. VII. In: Donovan AF, Lawrence HR, editors. High-Speed Aerodynamics and Jet Propulsion. Princeton, New Jersey: Princeton University Press; 1957. pp. 228-435

[23] Karafoli E. Aerodynamics of an Aircraft Wing. Moscow: AN USSR Publishing; 1956. 479 p. (In Russian)

[24] Ryzhkov UA. Approximate method of calculating forces acting on body in supersonic gas flow and problem of aerodynamic interference of wing-fuselage. In: Proceedings TsAGI; 1959. 759, pp. 24-37

[25] Lennertz J. On the mutual reaction of wings and body. NACA TM, 400; 1927

[26] Lennertz J. Beitrag zur theoretischen Behandlung des gegenseitigen Einflusses von Tragfläche und Rumpf. Abhandlungen aus dem Aerodyn. In: Durand WF, editor. Aerodynamics Vol. IV. Berlin: Springer; 1934

[27] Nikolsky AA. About lifting properties and induced drag of wing-fuselage system. In: Proceedings TsAGI; 1981. 2122, pp. 94-95

[28] Weber J. Interference problems on wing-fuselage combinations. Part I: Lifting unswept wing attached to a cylindrical fuselage at zero incidences in midwing position. RAE Technical Report 69130 (ARC 31532); 1969

[29] Weber J. Second-order small-perturbation theory for finite wings in incompressible flow. ARC R&M 3759; 1972

[30] Weber J, Joyce MG. Interference problems on wing-fuselage combinations Part III symmetrical swept wing at zero incidence attached to a cylindrical fuselage. ARC CP; 1975. 1333, p. 84

[31] Vernigora VN. Numerical study of interference of thin trapezoidal wing and cylindrical fuselage at subsonic speeds. In: Proceedings TsAGI; 1983. 2176, pp. 26-43

[32] Kholyavka VI. Interference of aircraft parts. Kharkiv: Aviation. Inst.; 1967. p. 107

[33] Ganiev FI, Urkova ME. Calculation results of aerodynamic characteristics of wing-body combination moving with high subsonic speed. In: Proceedings Air Force Academy named after Zhukovsky; 1971. 1302, pp. 220-241

[34] Kolesnikov GA. Calculation of aerodynamic characteristics of wing-body combination at unsteady motion. In: Proceedings TsAGI; 1961. 810, pp. 78-96

[35] Kolesnikov GA. Order and results of calculation of aerodynamic characteristics of wing-body combinations at unsteady motion. In: Proceedings TsAGI; 1965. 954, pp. 3-28

[36] Belotserkovsky SM, Skripach BK. Aerodynamic Derivatives Wing and the Aircraft at Subsonic Speeds. Moscow: Nauka; 1975. 424 p. (In Russian)

[37] Woodward FA. Analysis and design of wing-body combinations at subsonic and supersonic speeds. Journal of Aircraft. 1968;**5**(5):528-534

[38] Woodward FA. An improved method for the aerodynamic analysis of

wing-body-tail configuration in subsonic and supersonic flow. NASA CR-2228, Part I and Part II; 1973. pp. 126 and 315

[39] Cvitanović I, Virag Z, Krizmanić S. Analysis of potential flow around wing-body configurations. In: 4th International Congress of Croatian Society of Mechanics (4th ICCSM); 18-20 September 2003; Bizovac, Croatia; 2003. pp. 1-10

[40] Davari AR, Soltani MR, Askari F, Pajuhande HR. Effects of wing geometry on wing-body-tail interference in subsonic flow. Scientia Iranica. 2011;**18**(3):407-415

[41] Frolov VA. Methods for Calculating Lift for Wing-Body Combination. Saarbrucken: LAP Lambert Academic Publishing; 2011. 141 p. (in Russian)

[42] Frolov VA. Review results on wing-body. In: Proceedings of the International Conference on Mechanical, System and Control Engineering (ICMSE 2016); 18-20 May 2016; Moscow, Russia: MATEC Web of Conferences ICMIE; 2016. 75, 09006. DOI: 10.1051/matecconf/2016750900

[43] Milne-Thomson LM. Theoretical Aerodynamics. London: Constable and Company; 1958

[44] Mendenhall MR, Nielsen JN. Effect of symmetrical vortex shedding on the longitudinal aerodynamic characteristics of wing-body-tail combinations. NASA CR, 2473; 1975. p. 115

[45] Giesing JP, McDonnell-Douglas Rep. Douglas Aircraft Co., Report DAC, Vol. I, 67212. 1968

[46] Giesing JP, Kalman WP, Rodden WP. Subsonic unsteady aerodynamics for general configurations; Part I—Direct application of the nonplanar doublet-lattice method; Part II—Application of the doublet-lattice method and the method of images to lifting surface/body interference. USAF FDL-TR-71-5; 1971

[47] Martina AP. The interference effect of a body on the spanwise load distribution of two 45° sweptback wings of aspect ratio 8.02 from low-speed test NACA TN. 1956; p. 3730

[48] Gregoriou G. Zur gegenseitigen Beeinflussung eines endlich Langen Rumpfes und eines Flügels in Mitteldeckeranordnung bei Unterschallströmung. BMVg-FBWT-73-33; 1973

[49] Labrujere TE, Loeve W, Slooff JW. An approximate method for the calculation of pressure distribution on wing-body combinations at subcritical speeds. AGARD-CP, No. 071; 1970